Electronic Supplementary Information (ESI)

Greener Synthesis of 1,2,3-Triazoles using Copper (I)-Exchanged Magnetically Recoverable β-Zeolite as Catalyst

Elizama R. Costa,[a] Floyd C. D. Andrade,[a] Danilo Yano de Albuquerque,[a] Luanne E. M. Ferreira,[b] Thiago M. Lima,*[b] Carolina G. S. Lima,[c] Domingos S. A. Silva,[d] Ernesto A. Urquieta-González,[d] Márcio W. Paixão,[a] and Ricardo S. Schwab*[a]

[a] Centre of Excellence for Research in Sustainable Chemistry (CERSusChem), Departamento de Química, Universidade Federal de São Carlos - UFSCar, Rodovia Washington Luís, km 235 - SP-310, São Carlos, São Paulo, 13565-905, Brazil.
E-mail: rschwab@ufscar.br

[b] Departamento de Química Inorgânica, Universidade Federal Fluminense, Campus do Valonguinho, Outeiro São João Batista s/n, Centro, Niterói-RJ, 24020-150, Brazil.
E-mail:tmlima@id.uff.br

[c] Departamento de Química Orgânica, Universidade Federal Fluminense, Campus do Valonguinho, Outeiro São João Batista s/n, Centro, Niterói-RJ, 24020-150, Brazil.

[d] Research Center on Advanced Materials and Energy, Universidade Federal de São Carlos (DEQ), C. Postal 676, 13565-905, São Carlos, SP, Brazil

Table of Contents

1. Experimental

1.1 Materials and Methods

Hydrogen nuclear magnetic resonance spectra (^{1}H NMR) were obtained, on Bruker Advance 400 MHz spectrometer. ^{1}H NMR spectra were referenced to the residual hydrogen signal in $CDCl_3$ at $\delta = 7.26$ ppm. Coupling constants (*J*) are reported in Hertz [Hz] using the standard notation to described the multiplicity of signals. Carbon-13 nuclear magnetic resonance spectra (^{13}C NMR) were obtained at 101 MHz. ^{13}C spectra were referenced to the $CDCl_3$ triplet signal at $\delta = 77.0$ ppm. Flash column chromatography was performed using Merck Silica Gel (230-400 mesh). Thin layer chromatography (TLC) was performed using Merck Silica Gel GF254, 0.25 mm thickness. For visualization, TLC plates were either placed under short wave ultraviolet light (254 nm), stained with iodine vapor, or acidic vanillin. The yields of the products included in all tables refer to isolated yields. All commercially available reagents were purchased at the highest commercial quality and used without further purification, unless otherwise noted.

The particle size and morphological studies of the Fe_3O_4 microspheres used as support and the catalysts were performed by Transmission Electron Microscopy (TEM), which was carried out using a FEI TECNAI G2 F20 microscope. For the TEM analyses, the powder samples were dispersed in ethanol and sonicated for 5 min. One drop of this solution was placed on a 400 mesh nickel grid with carbon film and the sample was dried at room temperature.

The XRD measurements were performed in a Shimadzu XRD 6000 Diffractometer using the Kα radiation of a Cu source (λ=1.54056 Å), 40 kV, 30 mA and 2θ in the range of 5° to 80° and a rate of 2° min^{-1}.

X-ray Photoelectron Spectroscopy (XPS) was performed using a Scienta Omicron ESCA+ spectrometer with a high-performance hemispheric analyzer (EA 125) with monochromatic Al Kα (hν = 1486.6 eV) radiation as the excitation source. The operating pressure in the ultrahigh vacuum chamber (UHV) during analysis was $2x10^{-9}$ mbar. Energy steps of 50 and 20 eV were used for the survey and high-resolution spectra, respectively. TPD measurements were conducted in a Micromeritics Autochem II 2920 Chemisorption Analyzer equipment with a TCD (Thermal Conductivity Detector) detector. Fifty miligrams of the sample were pre-treated under 30 mL min^{-1} of He flow at a heating rate of 10 °C min^{-1} until 500 °C and kept at this temperature for 30 minutes. After this period, the reactor was cooled to 120 °C, and the He flow was kept for 60 minutes.

ICP-OES measurements were conducted in a Thermo Fisher Scientific, iCAP 6300 Duo, with a CID (Charge Injection Device) detector.

The magnetic measurements were carried out using and apparatus combining a superconducting quantum interference device and a vibrating sample magnetometer model Quantum Design MPMS SQUID-VSM. The magnetization was measured as function of the applied magnetic field (MxH) at room temperature and up to 70 kOe.

Thermogravimetric analyses were performed in a Shimadzu, thermogravimetric module TGA-50.

The textural properties of the materials were determined by nitrogen physisorption measurements at -196°C at a Micromeritics equipment (ASAP-2420). Previously to the analyses, the samples were treated under vacuum at 90 °C for 30 minutes and 200 °C for 6 h in order to eliminate water and physically adsorbed gases. The pore size distribution was calculated using the Barrett-Joyner-Halenda (BJH) model, and the specific surface area was calculated using the BET equation. The micropore volume and external area were estimated through the t-plot method using Halsey's equation. The total micropore volume was calculated at $p/p_o = 0.98$.

The FT-IR analyses were conducted in the transmission mode using KBr as a dillutant. The pellet containing 1% (m/m) of the sample was analyzed in a Bruker Vertex 70 spectrometer equipped with a L-alanine and deuterium-dopped triglycine sulfate dectector. The spectrum was collected in the range of 400 to 4000 cm^{-1} with a resolution of 4 cm^{-1}.

1.2. General Procedure for the 1,3-Dipolar Cycloaddition Reaction

Typical procedure:

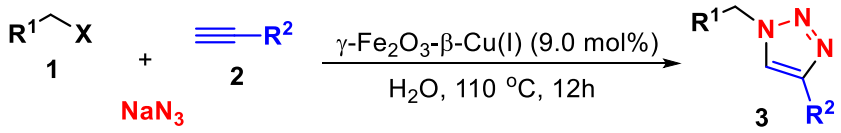

In an Ace® pressure tube, the γ-Fe_2O_3-β-Cu(I) catalyst (9.0 mol%), alkyl halide (0.5 mmol), sodium azide (0.5 mmol), alkyne (0.5 mmol), and 3.0 mL of water were added. The reaction tube was sealed and heated in oil bath at 110°C and magnetically stirred for 12 h. After the completion of the reaction and separation of catalyst with the aid of a permanent magnet, the product was extracted from the catalyst by washing with ethyl

acetate. The solvents and volatiles were completely removed under vacuum to give the crude product. The resulting crude compound was purified by flash column chromatography on silica gel (hexane:ethyl acetate, 7:3). The catalyst was then washed with ethyl acetate, water and ethanol, dried at 100°C for 12 h and reused in a subsequent reaction run. The isolated product was then subjected to ^{1}H NMR and ^{13}C NMR.

2. Characterization data

2.1 Catalyst characterization

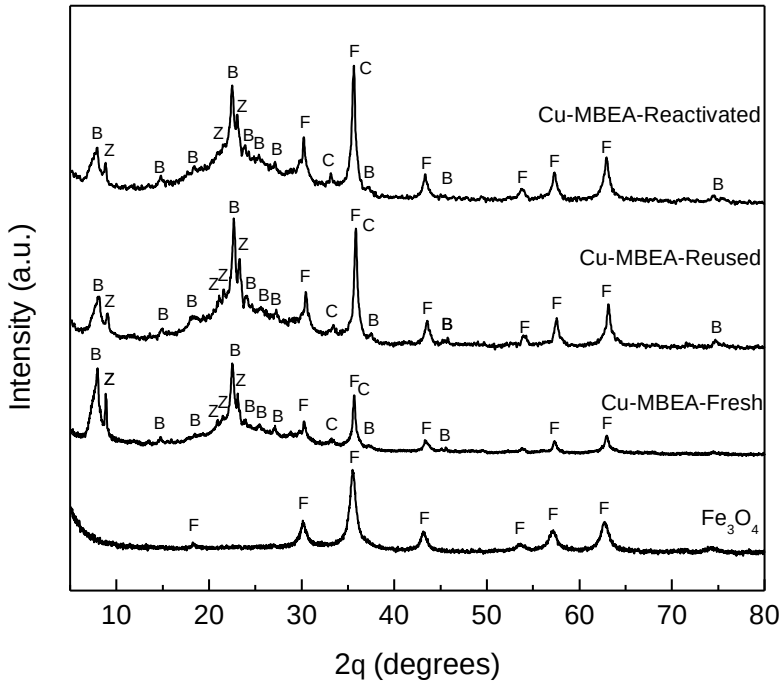

Figure S1. XRD diffractograms of Fe_3O_4 nanoparticles and magnetically recoverable copper-exchanged beta zeolite catalysts (F: Fe_3O_4/γ-Fe_2O_3; B: β-zeolite; Z: ZSM-12 zeolite; C: CuO)

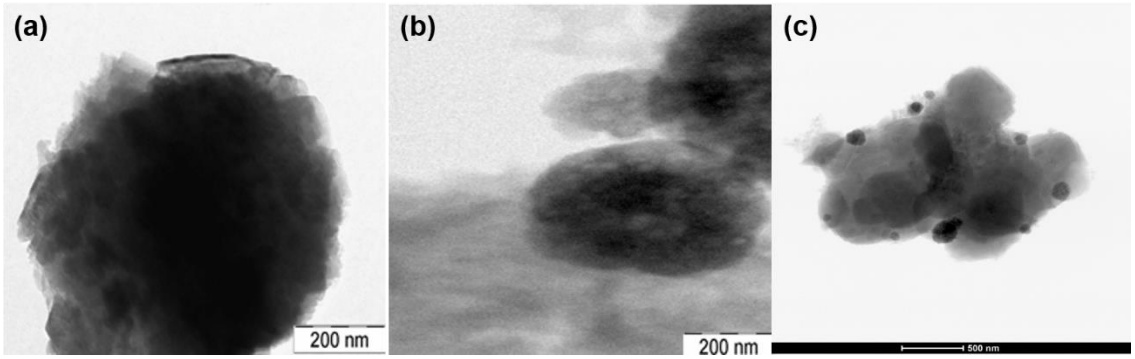

Figure S2. TEM images of (a) pure β-zeolite, (b) γ-Fe_2O_3-β-Na^+ and (c) γ-Fe_2O_3-β-Cu(I).

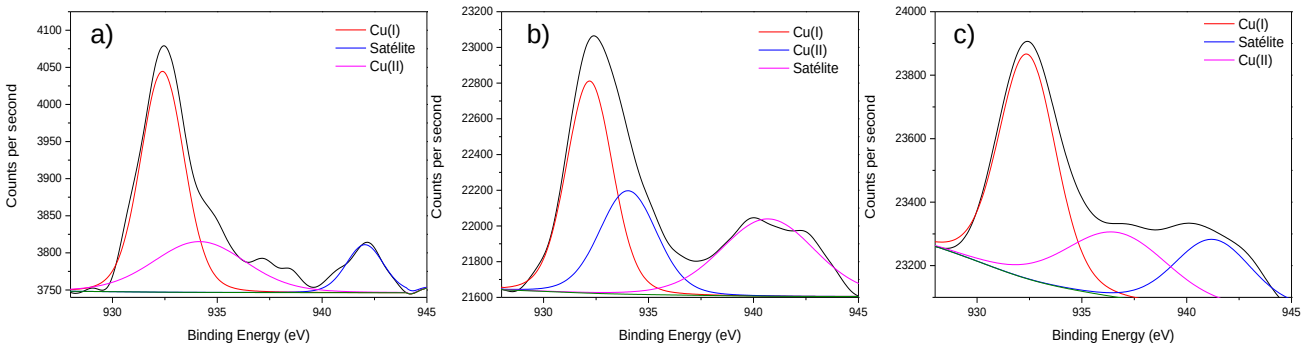

Figure S3. XPS spectra of a) the fresh, b) the deactivated and c) the reactivated catalysts γ-Fe_2O_3-β-Cu(I).

Table S1. Relative quantitative amount of each Cu components in the XPS spectrum of copper exchanged magnetically recoverable beta zeolite.

Catalyst	Component	Position (eV)	FWHM	Concentration (%)
Fresh catalyst	Cu^+ species	932.39	2.45	59.8
	Cu^{2+} species	934.15	5.18	29.1
	Cu^{2+} satellite	942.04	2.09	11.1
Catalyst after 7th reaction run	Cu^+ species	932.19	2.58	42.6
	Cu^{2+} species	934.02	5.23	31.5
	Cu^{2+} satellite	940.69	3.20	25.8
Recalcined catalyst	Cu^+ species	932.489	3.19	51.7
	Cu^{2+} species	936.68	5.79	27.0
	Cu^{2+} satellite	941.24	4.32	21.3

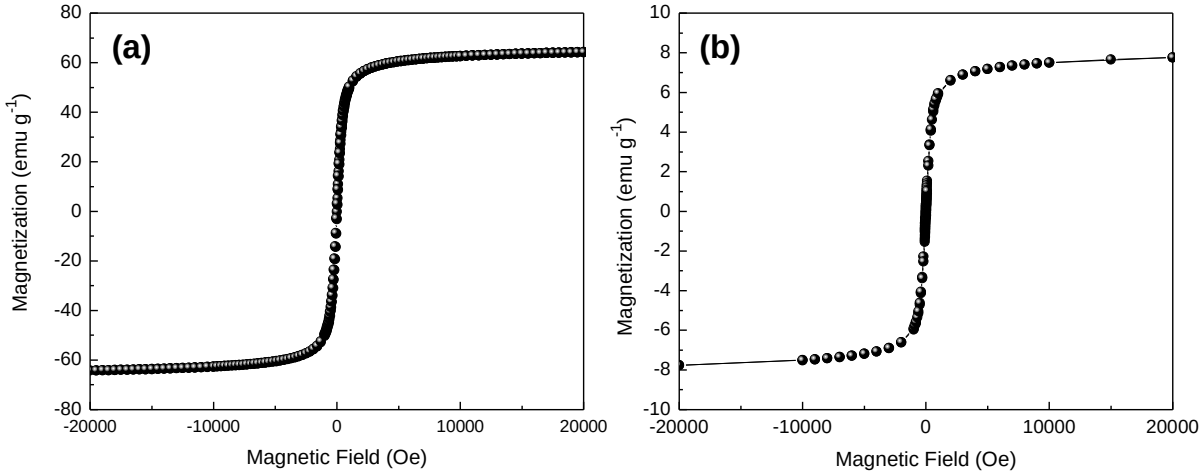

Figure S4. SQUID magnetization curves of (a) Fe_3O_4 microspheres and (b) copper exchanged magnetically recoverable beta zeolite [γ-Fe_2O_3-β-Cu(I)].

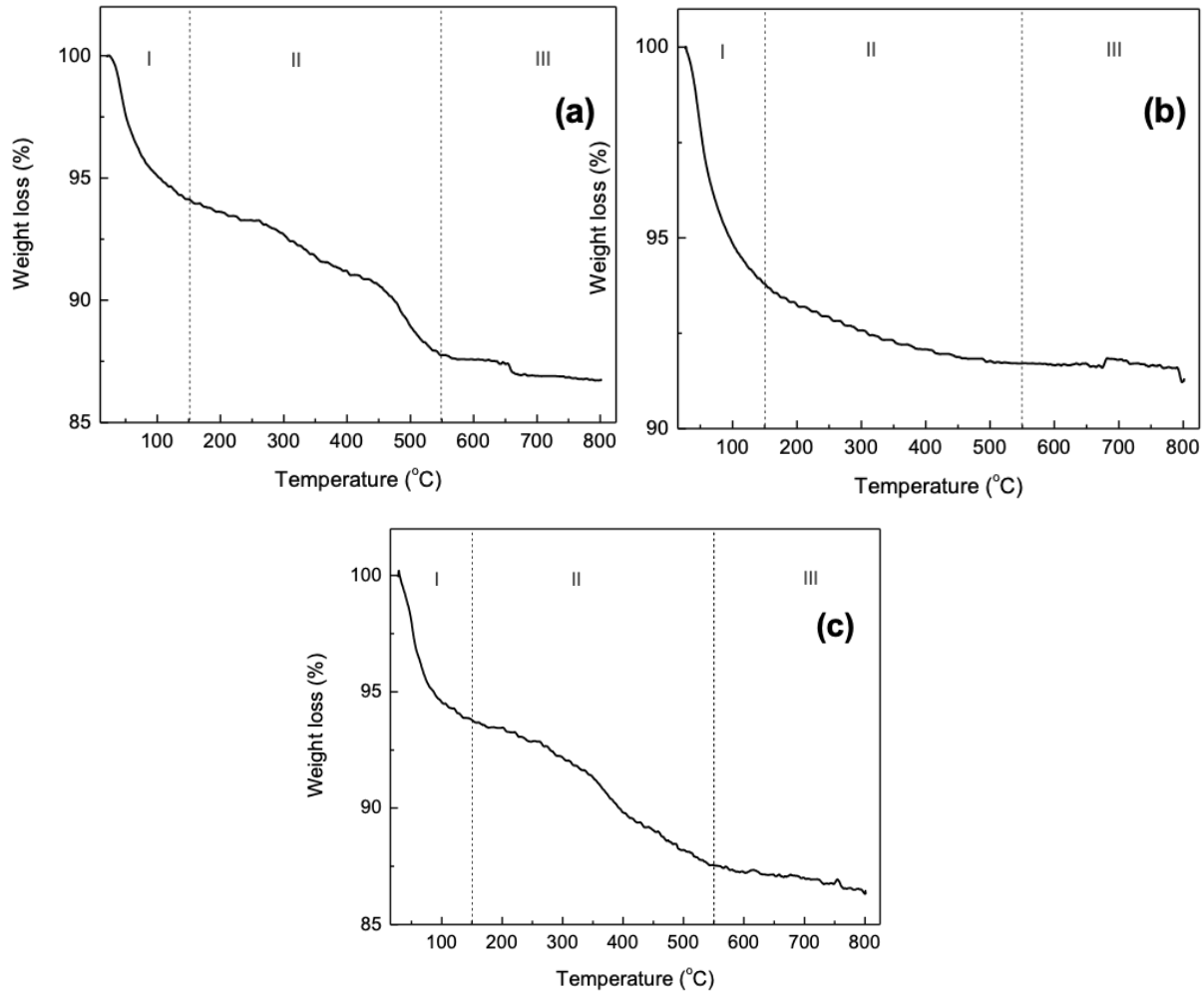

Figure S5. Thermogravimetric curves of (a) deactivated catalyst after 7th reuse (b) reactivated catalyst after calcination under 550 ^{o}C for 3 h and (c) catalyst after the 8th reaction run.

Table S2. Weight loss assigned to the steps in the curves of the Figure S4.

Catalyst	Weight loss step	Temperature range	Weight loss %
Catalyst after 7th reaction run	1st step	25-150 °C	5.896
	2nd step	150-550 °C	6.407
Reactivated catalyst	1st step	25-150 °C	6.231
	2nd step	150-550 °C	2.000
Catalyst after 8th reaction run	1st step	25-150 °C	6.232
	2nd step	150-550 °C	6.247

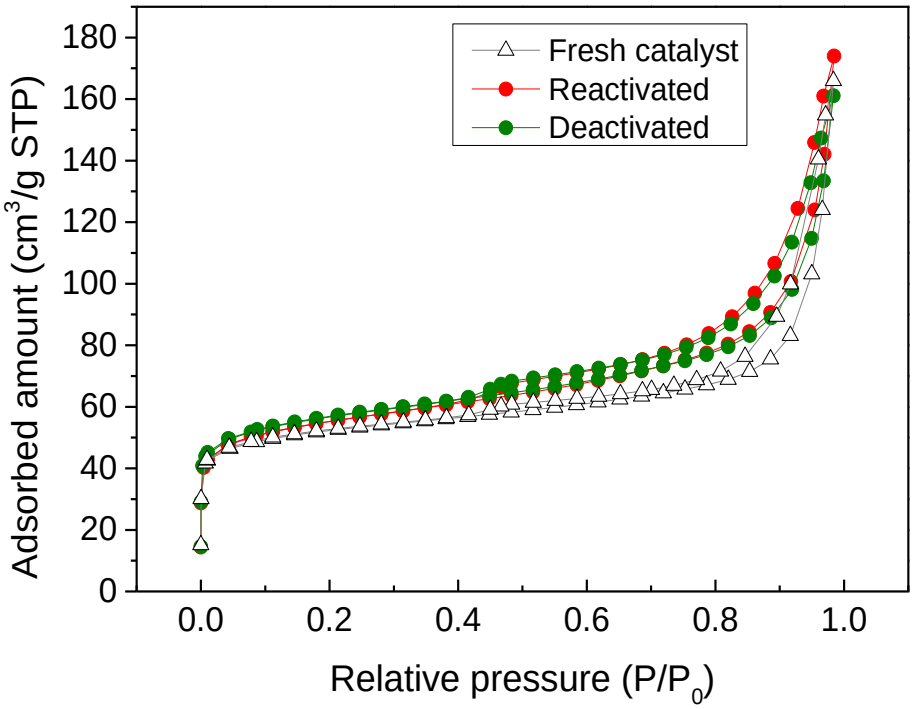

Figure S6. Nitrogen physisorption isotherms of the fresh, deactivated after 7th reaction run and reactivated catalyst after thermal treatment (550 °C for 3 h).

Table S3. Textural properties of the fresh, deactivated after 7th run and reactivated after thermal treatment.

Sample	$S_{External}$ (m^2 g^{-1})	S_{BET} (m^2 g^{-1})	$V_{Micropore}$ (m^3 g^{-1})	V_{Toral} (m^3 g^{-1})*
Fresh catalyst	52	196	0.06	0.24
Deactivated after 7th run	78	202	0.05	0.25
Reactivated after thermal treatment	71	210	0.05	0.24

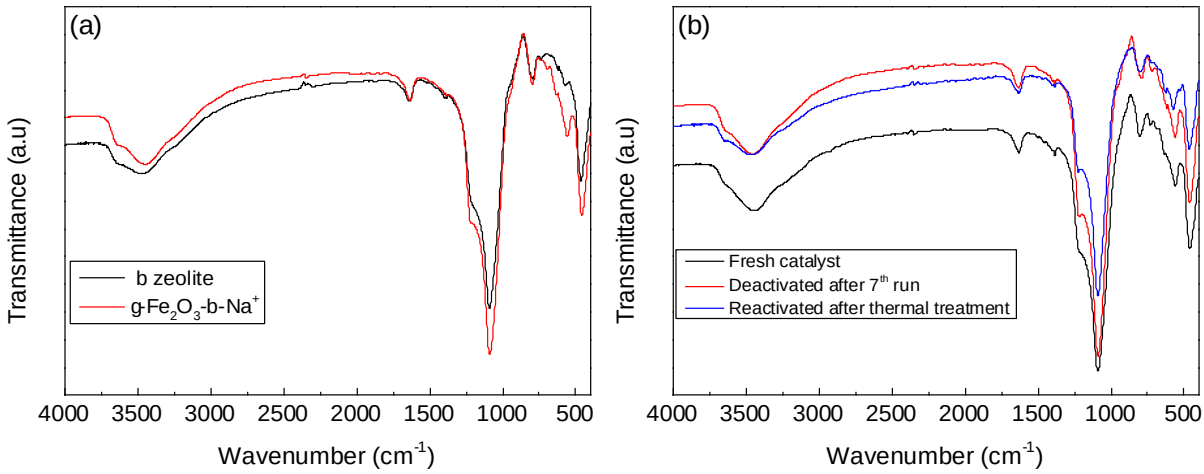

Figure S7. FT-IR spectra of a) β-zeolite in the sodium form and the magnetically recoverable β-zeolite in the sodium form and b) the fresh and spent catalysts.

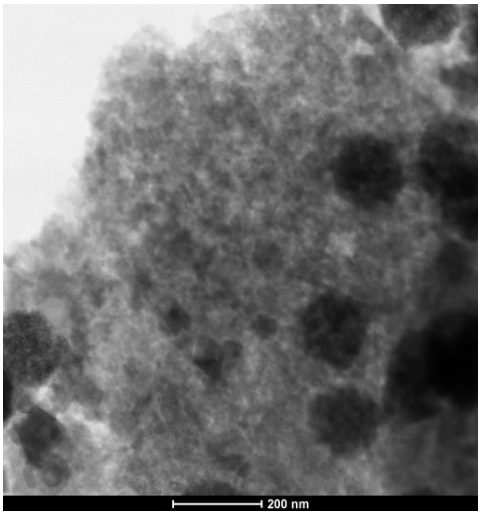

Figure S8. TEM image of the reactivated catalyst γ-Fe_2O_3-β-Cu(I) after the calcination procedure.

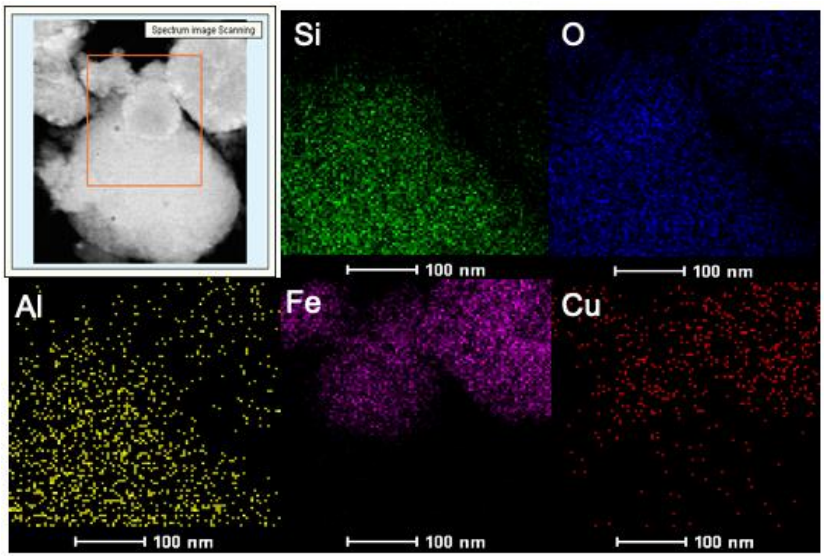

Figure S9. TEM image and chemical mapping of the reactivated catalyst γ-Fe_2O_3-β-Cu(I) after the calcination procedure.

2.2 Characterization data of 1,4-dissubstituted 1,2,3-triazoles

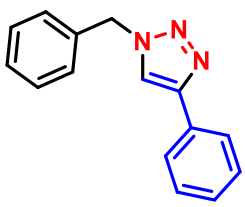

1-benzyl-4-phenyl-1H-1,2,3-triazole (**3a e 3b**): **^{1}H NMR** (400 MHz, $CDCl_3$) δ 7.86-7.78 (m, 2H), 7.66 (s, 1H), 7.50-7.38 (m, 5H), 7.36-7.29 (m, 3H), 5.58 (s, 2H). **^{13}C NMR** (101 MHz, $CDCl_3$) δ 148.22, 134.73, 130.48, 129.26, 128.92, 128.33, 128.17, 125.83, 119.70, 54.37.

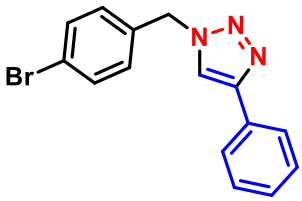

1-(4-bromobenzyl)-4-phenyl-1H-1,2,3-triazole (**3c**): **^{1}H NMR** (400 MHz, $CDCl_3$) δ 7.80 (d, *J* = 8.3 Hz, 1H), 7.67 (s, 1H), 7.51 (d, *J* = 8.3 Hz, 1H), 7.40 (t, *J* = 7.4 Hz, 1H), 7.32 (t, *J* = 7.3 Hz, 1H), 7.17 (d, *J* = 8.2 Hz, 1H), 5.52 (s, 1H). **^{13}C NMR** (101 MHz, $CDCl_3$) δ 148.40, 137.84, 133.66, 132.37, 130.26, 129.68, 128.87, 128.35, 125.75, 123.01, 119.47, 53.61.

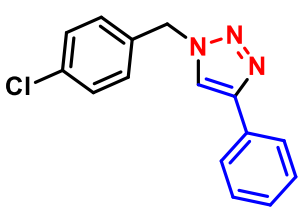

1-(4-chlorobenzyl)-4-phenyl-1H-1,2,3-triazole (**3d**): **^{1}H NMR** (400 MHz, $CDCl_3$) δ 7.82-7.78 (m, 2H), 7.66 (s, 1H), 7.45-7.30 (m, 6H), 7.25 (d, *J* = 9.1 Hz, 3H), 5.55 (s, 2H). **^{13}C NMR** (101 MHz, $CDCl_3$) δ

148.52, 134.98, 133.31, 130.47, 129.50, 128.98, 128.42, 125.84, 119.56, 53.61.

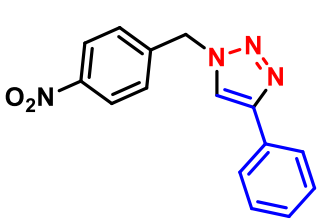

1-(4-nitrobenzyl)-4-phenyl-1H-1,2,3-triazole (**3e**): **^{1}H NMR** (400 MHz, $CDCl_3$) δ 8.24 (d, *J* = 8.7 Hz, 2H), 7.81 (d, *J* = 8.6 Hz, 2H), 7.76 (s, 1H), 7.48-7.38 (m, 4H), 7.34 (tt, *J* = 6.3, 1.4 Hz, 1H), 5.70 (s, 2H). **^{13}C NMR** (101 MHz, $CDCl_3$) δ 148.88, 148.24, 141.86, 130.21, 129.06, 128.68, 128.64, 125.88, 124.50, 119.80, 53.33.

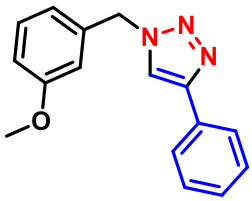

1-(3-methoxybenzyl)-4-phenyl-1H-1,2,3-triazole (**3f**): **^{1}H NMR** (400 MHz, $CDCl_3$) δ 7.81-7.78 (m, 2H), 7.67 (s, 1H), 7.41-7.37 (m, 2H), 7.33-7.26 (m, 2H), 6.90-6.88 (m, 2H), 6.83-6.82 (m, 2H), 5.53 (s, 2H), 3.77 (s, 3H). **^{13}C NMR** (101 MHz, $CDCl_3$) δ 160.24, 148.32, 136.23, 130.63, 130.34, 128.91, 128.27, 125.80, 120.35, 119.64, 114.34, 113.75, 55.42, 54.26.

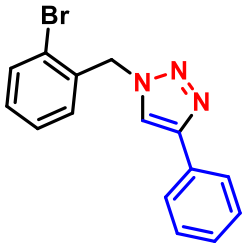

1-(2-bromobenzyl)-4-phenyl-1H-1,2,3-triazole (**3g**): **^{1}H NMR** (400 MHz, $CDCl_3$) δ 7.84-7.80 (m, 2H), 7.79 (s, 1H), 7.63 (dd, *J* = 7.9, 1.2 Hz, 1H), 7.44-7.36 (m, 2H), 7.36-7.28 (m, 2H), 7.26 – 7.17 (m, 2H), 5.71 (s, 2H). **^{13}C NMR** (101 MHz, $CDCl_3$) δ 134.21, 133.25, 130.46, 130.31, 128.85, 128.29, 125.77, 123.44, 119.86, 53.92.

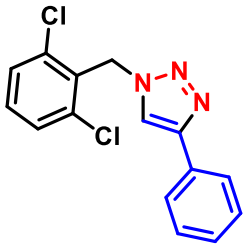

1-(2,6-dichlorobenzyl)-4-phenyl-1H-1,2,3-triazole (**3h**): **^{1}H NMR** (400 MHz, $CDCl_3$) δ 7.80 (d, *J* = 7.3 Hz, 2H), 7.70 (s, 1H), 7.46-7.36 (m, 4H), 7.35-7.28 (m, 2H), 5.91 (s, 2H). **^{13}C NMR** (101 MHz, $CDCl_3$) δ 147.68, 136.87, 131.15, 130.40, 130.12, 128.96, 128.79, 128.19, 125.76, 119.28, 49.14.

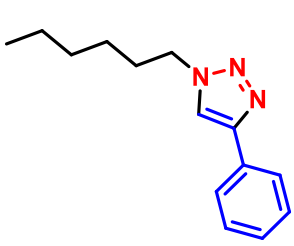

1-hexyl-4-phenyl-1H-1,2,3-triazole (**3i**): **^{1}H NMR** (400 MHz, $CDCl_3$) δ 7.86 – 7.81 (m, 1H), 7.76 (s, 1H), 7.44-7.38 (m, 1H), 7.35-7.29 (m, 1H), 4.38 (t, *J* = 7.2 Hz, 1H), 2.00-1.88 (m, 1H), 1.38-1.27 (m, 3H), 0.95-0.82 (m, 2H). **^{13}C NMR** (101 MHz, $CDCl_3$) δ 147.66, 130.59, 128.85, 128.14, 125.72, 119.50, 50.51, 31.17, 30.31, 26.17, 22.42, 13.96.

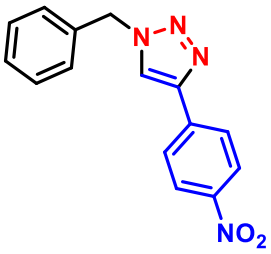

1-benzyl-4-(4-nitrophenyl)-1H-1,2,3-triazole (**3j**): **^{1}H NMR** (400 MHz, $CDCl_3$) δ 8.27 (d, *J* = 9.0 Hz, 2H), 7.97 (d, *J* = 9.0 Hz, 2H), 7.79 (s, 1H), 7.45-7.38 (m, 3H), 7.36-7.31 (m, 2H), 5.61 (s, 2H). **^{13}C NMR** (101 MHz, $CDCl_3$) δ 147.43, 146.15, 136.90, 134.27, 129.44, 129.21, 128.33, 126.26, 124.41, 121.09, 54.62.

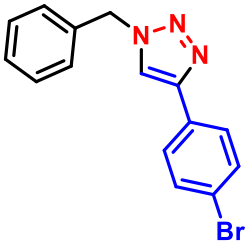

1-benzyl-4-(4-bromophenyl)-1H-1,2,3-triazole (**3k**): **^{1}H NMR** (400 MHz, $CDCl_3$) δ 7.67 (d, *J* = 8.7 Hz, 1H), 7.65 (s, 1H), 7.52 (d, *J* = 8.7 Hz, 1H), 7.43-7.35 (m, 2H), 7.34-7.29 (m, 1H), 5.57 (s, 1H). **^{13}C NMR** (101 MHz, $CDCl_3$) δ 147.14, 134.43, 131.98, 129.37, 129.24, 128.93, 128.15, 127.26, 122.14, 119.61, 54.39.

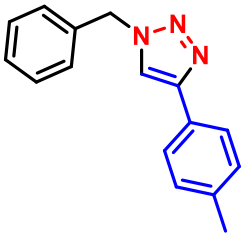

1-benzyl-4-(p-tolyl)-1H-1,2,3-triazole (**3l**): **^{1}H NMR** (400 MHz, $CDCl_3$) δ 7.69 (d, *J* = 8.1 Hz, 1H), 7.62 (s, 1H), 7.42-7.35 (m, 1H), 7.33-7.29 (m, 1H), 7.21 (d, *J* = 7.9 Hz, 1H), 5.57 (s, 1H), 2.36 (s, 2H). **^{13}C NMR** (101 MHz, $CDCl_3$) δ 148.11, 138.22, 134.57, 129.53, 129.18, 128.84, 128.12, 127.33, 125.70, 119.28, 54.38, 21.29.

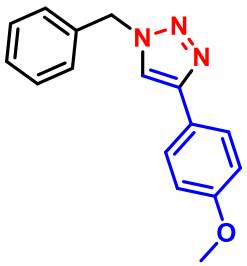

1-benzyl-4-(4-methoxyphenyl)-1H-1,2,3-triazole (**3m**): **^{1}H NMR** (400 MHz, $CDCl_3$) δ 7.72 (d, *J* = 8.9 Hz, 2H), 7.57 (s, 1H), 7.40-7.35 (m, 3H), 7.33-7.28 (m, 2H), 6.93 (d, *J* = 8.9 Hz, 2H), 5.56 (s, 2H), 3.83 (s, 3H). **^{13}C NMR** (101 MHz, $CDCl_3$) δ 159.73, 148.25, 134.90, 129.28, 128.89, 128.19, 127.14, 123.40, 118.81, 114.34, 55.46, 54.35.

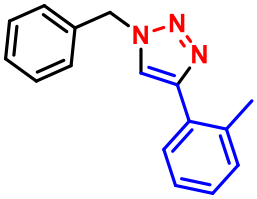

1-benzyl-4-(o-tolyl)-1H-1,2,3-triazole (**3n**): **^{1}H NMR** (400 MHz, $CDCl_3$) δ 7.77-7.72 (m, 1H), 7.56 (s, 1H), 7.42-7.35 (m, 3H), 7.33-7.29 (m, 2H), 7.25 (dd, *J* = 3.4, 2.3 Hz, 3H), 5.61 (s, 2H), 2.43 (s, 3H). **^{13}C NMR** (101 MHz, $CDCl_3$) δ 147.69, 135.61, 134.92, 130.97, 129.98, 129.26, 129.00, 128.86, 128.27, 1285.09, 126.17, 121.78, 54.27, 21.50.

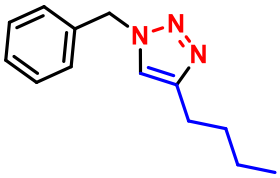

1-benzyl-4-butyl-1H-1,2,3-triazole (**3o**): **^{1}H NMR** (400 MHz, $CDCl_3$) δ 7.32-7.27 (m, 1H), 7.20-7.17 (m, 1H), 7.13 (s, 1H), 5.42 (s, 1H), 2.71-2.53 (m, 1H), 1.55 (ddd, *J* = 12.9, 8.5, 6.5 Hz, 1H), 1.29 (dq, *J* = 14.6, 7.4 Hz, 1H), 0.84 (t, *J* = 7.4 Hz, 1H). **^{13}C NMR** (101 MHz, $CDCl_3$) δ 148.82, 134.87, 129.08, 128.66, 127.99, 120.60, 54.09, 31.47, 25.32, 22.31, 13.80.

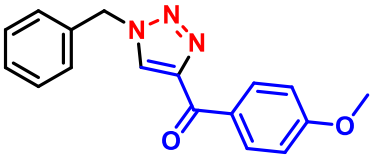

(1-benzyl-1H-1,2,3-triazol-4-yl)(4-methoxyphenyl)methanone (**3q**): **^{1}H NMR** (400 MHz, $CDCl_3$) δ 8.50 (d, *J* = 9.0 Hz, 2H), 8.14 (s, 1H), 7.44-7.38 (m, 3H), 7.35-7.31 (m, 2H), 6.99 (d, *J* = 9.0 Hz, 2H), 5.60 (s, 2H), 3.89 (s, 3H). **^{13}C NMR** (101 MHz, $CDCl_3$) δ 184.04, 163.95, 148.94, 133.88, 133.25, 129.46, 129.28, 128.51, 128.25, 113.81, 55.64, 54.58.

3. ^{1}H and ^{13}C NMR Spectra of the 1,4-dissubstituted 1,2,3-triazoles

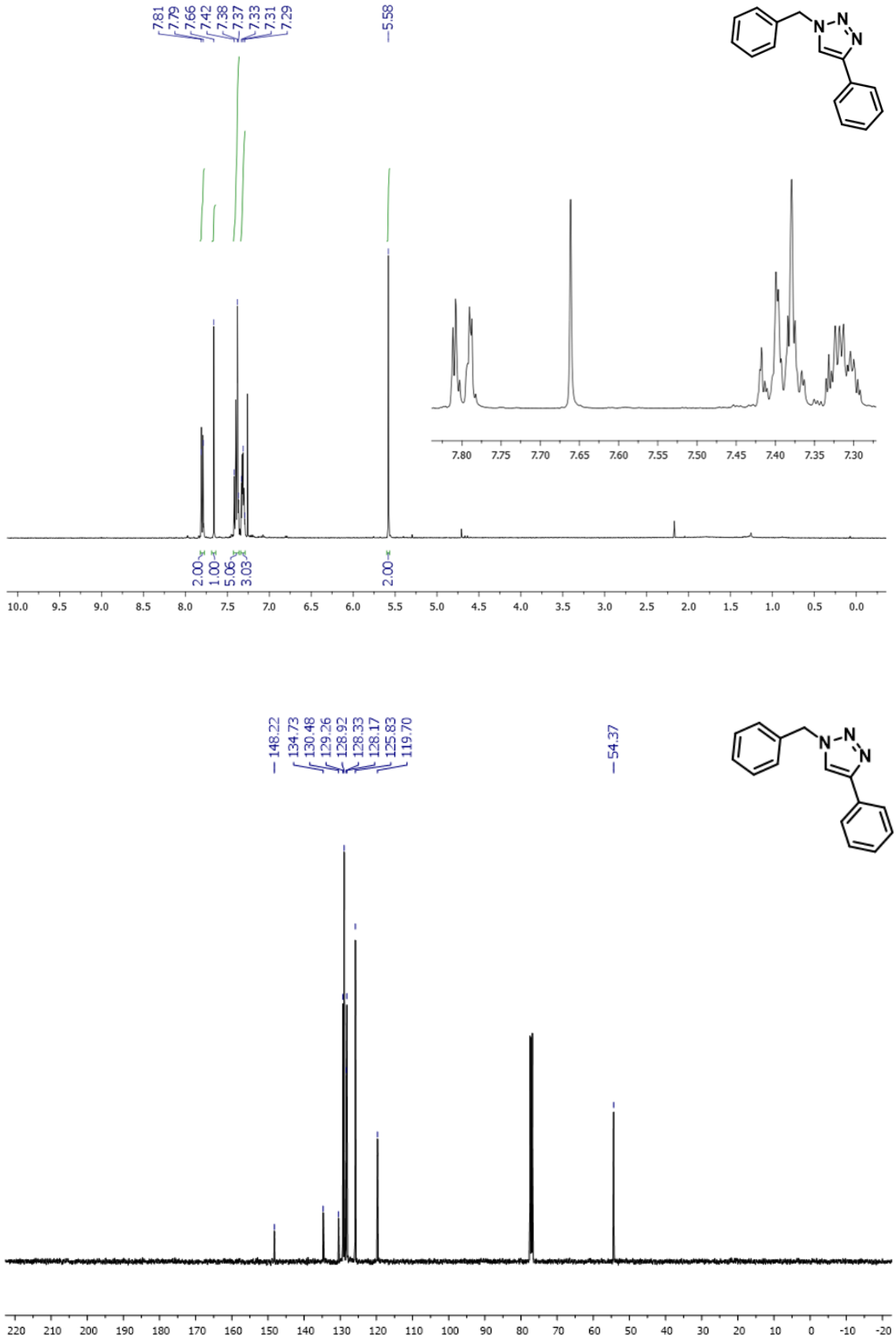

Figure 1. ^{1}H and ^{13}C NMR spectra in $CDCl_3$ of compound **3a**.

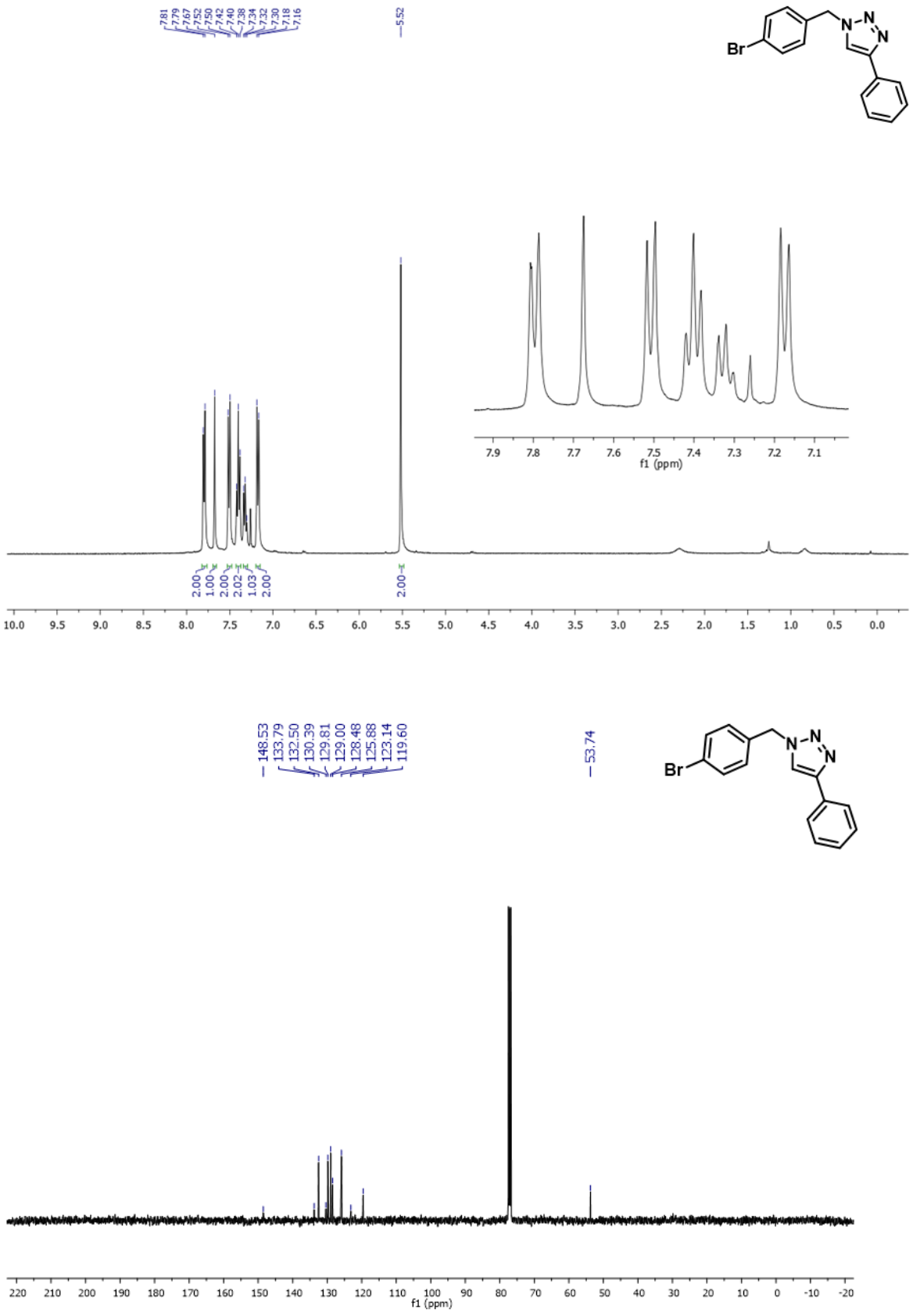

Figure 2. ^{1}H and ^{13}C NMR spectra in $CDCl_3$ of compound **3c**.

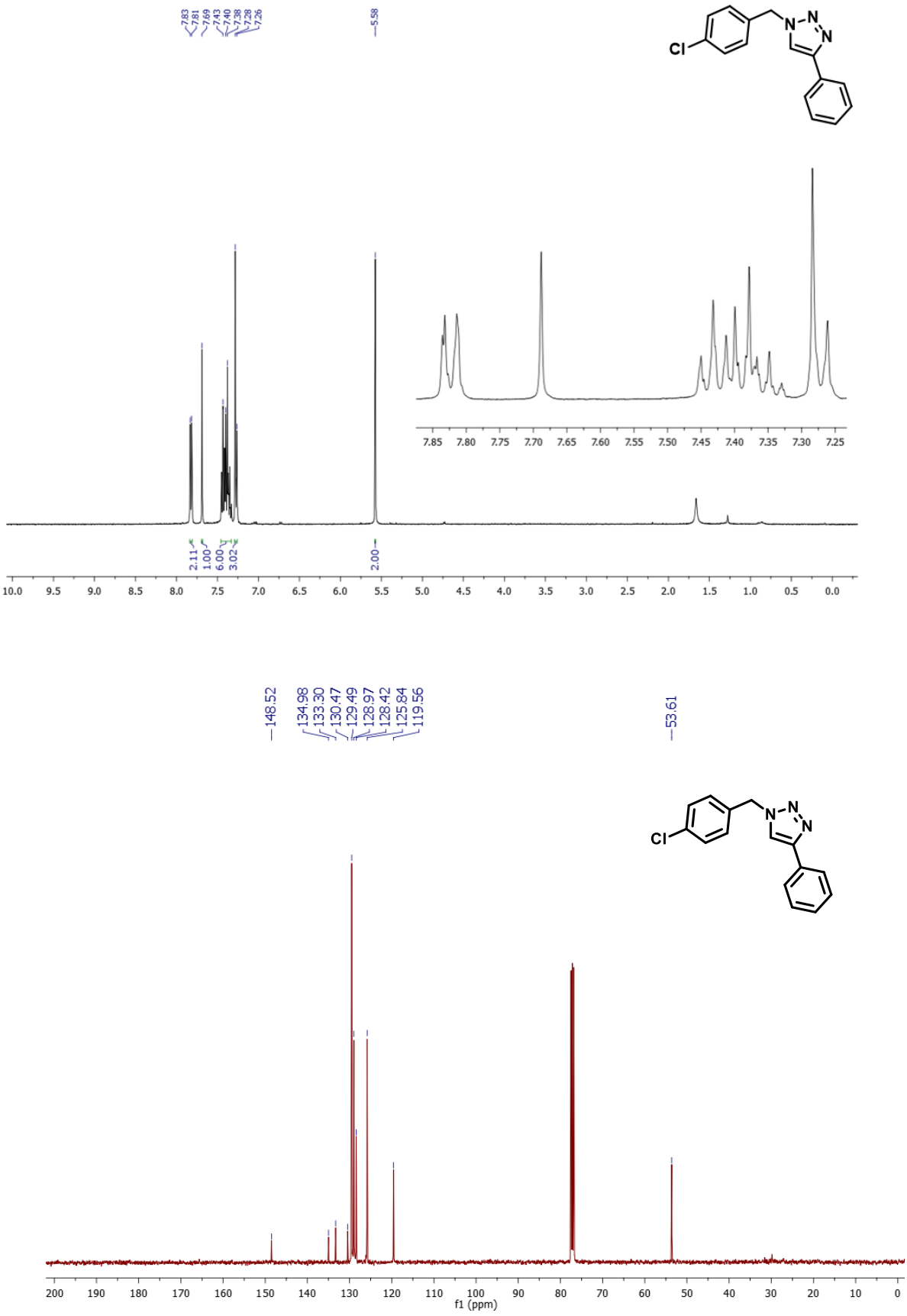

Figure 3. ^{1}H and ^{13}C NMR spectra in $CDCl_3$ of compound **3d**.

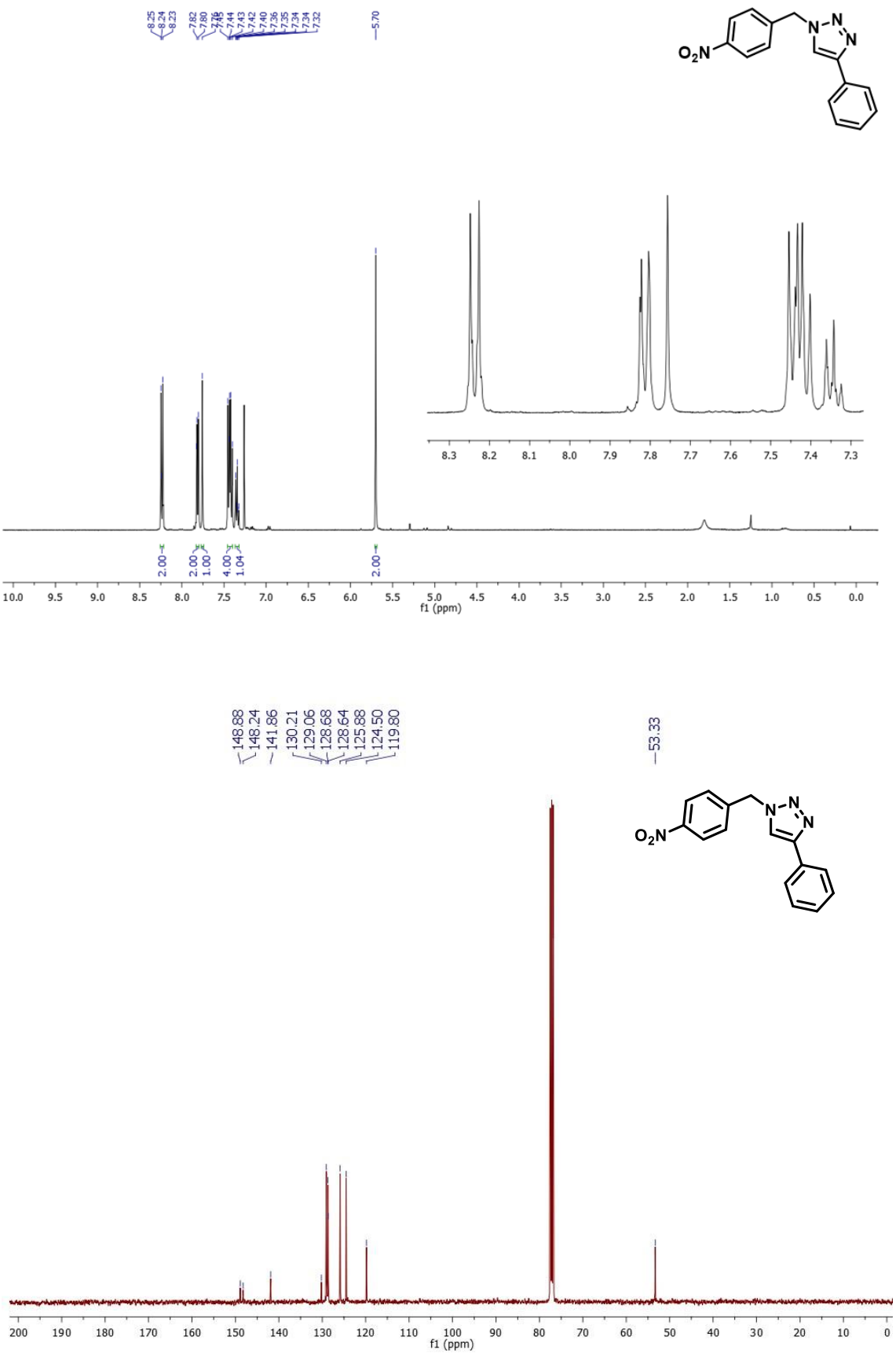

Figure 4. ^{1}H and ^{13}C NMR spectra in $CDCl_3$ of compound **3e**.

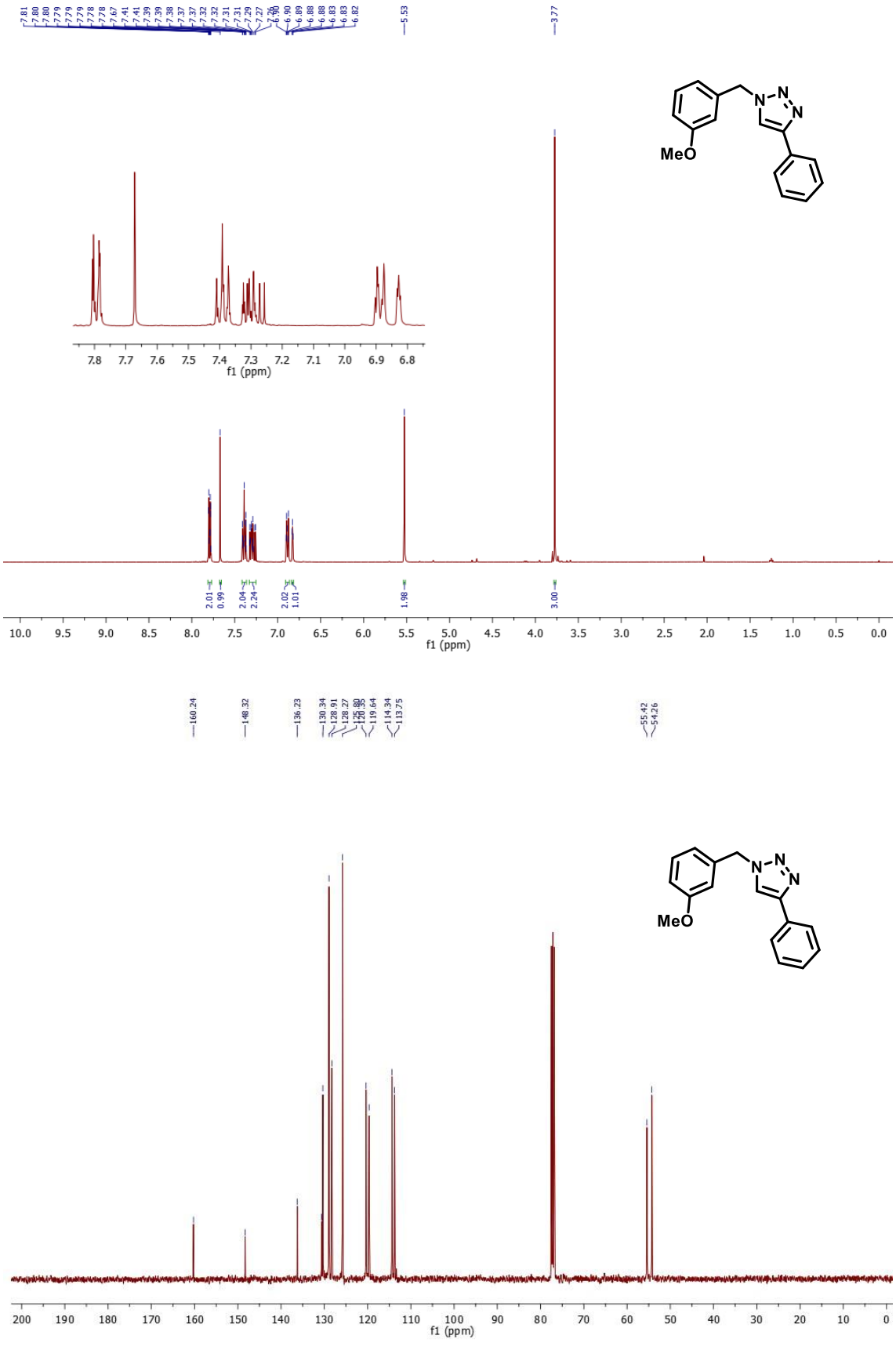

Figure 5. ^{1}H and ^{13}C NMR spectra in $CDCl_3$ of compound **3f**.

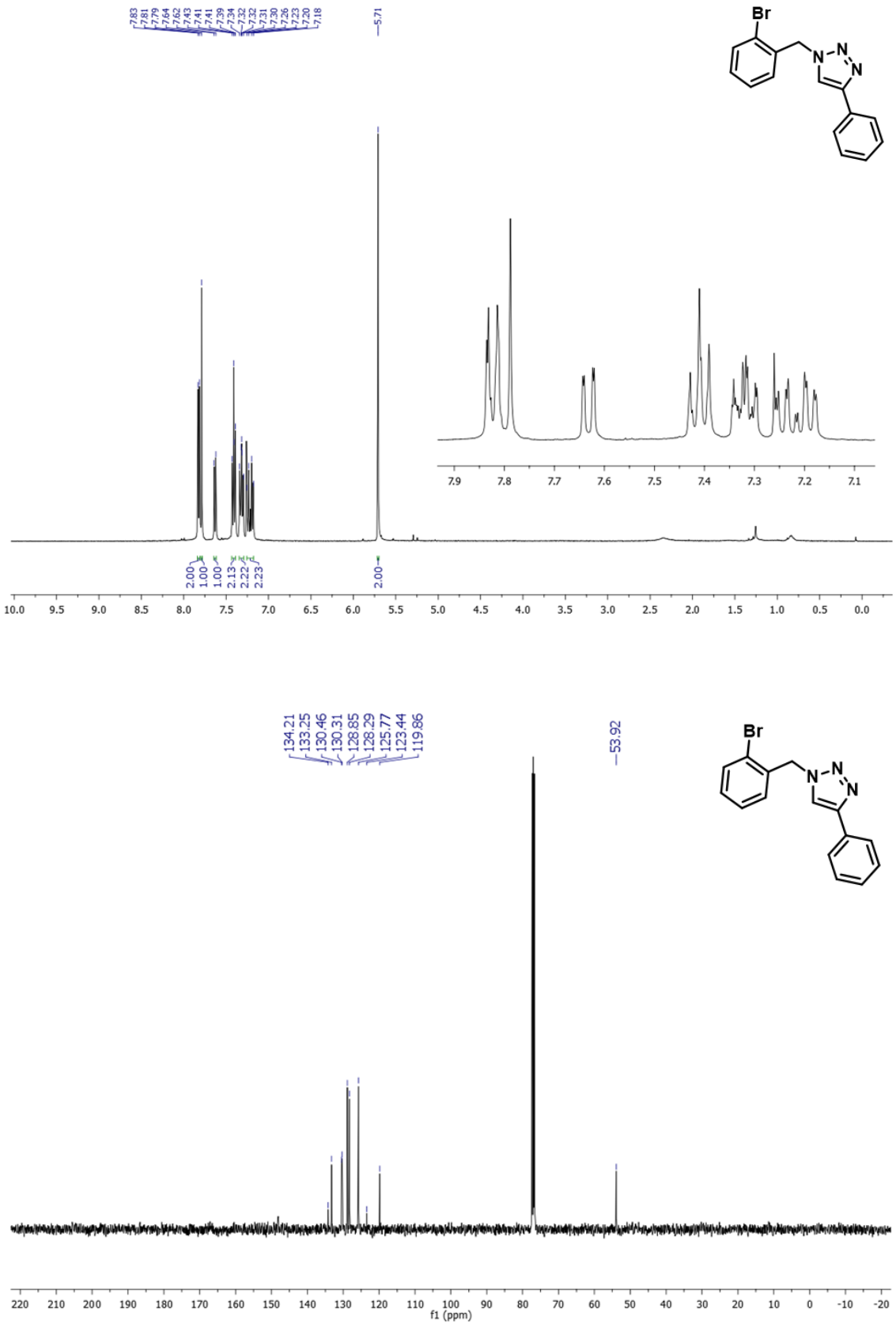

Figure 6. ^{1}H and ^{13}C NMR spectra in $CDCl_3$ of compound **3g**.

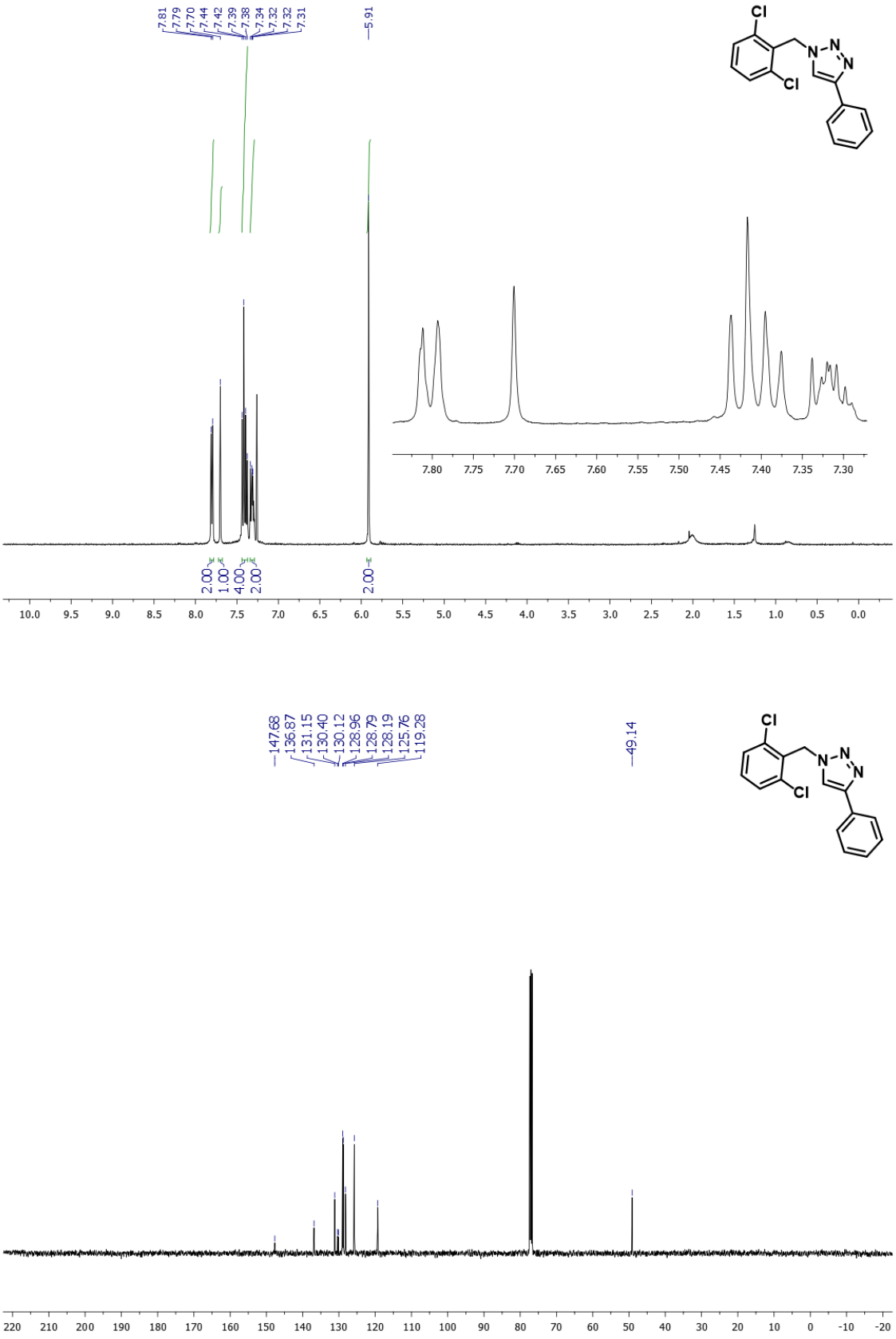

Figure 7. ^{1}H and ^{13}C NMR spectra in $CDCl_3$ of compound **3h**.

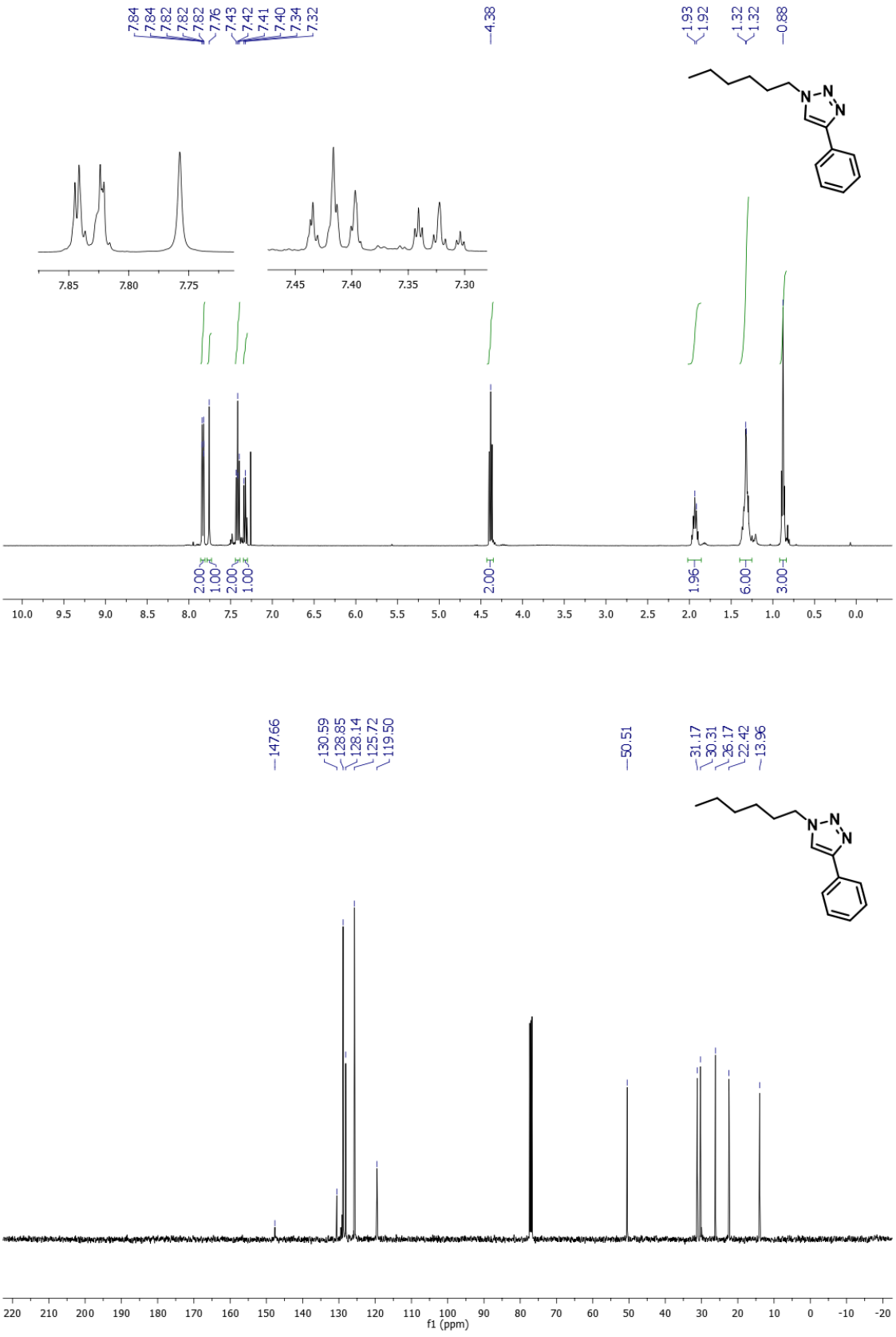

Figure 8. ^{1}H and ^{13}C NMR spectra in $CDCl_3$ of compound **3i**.

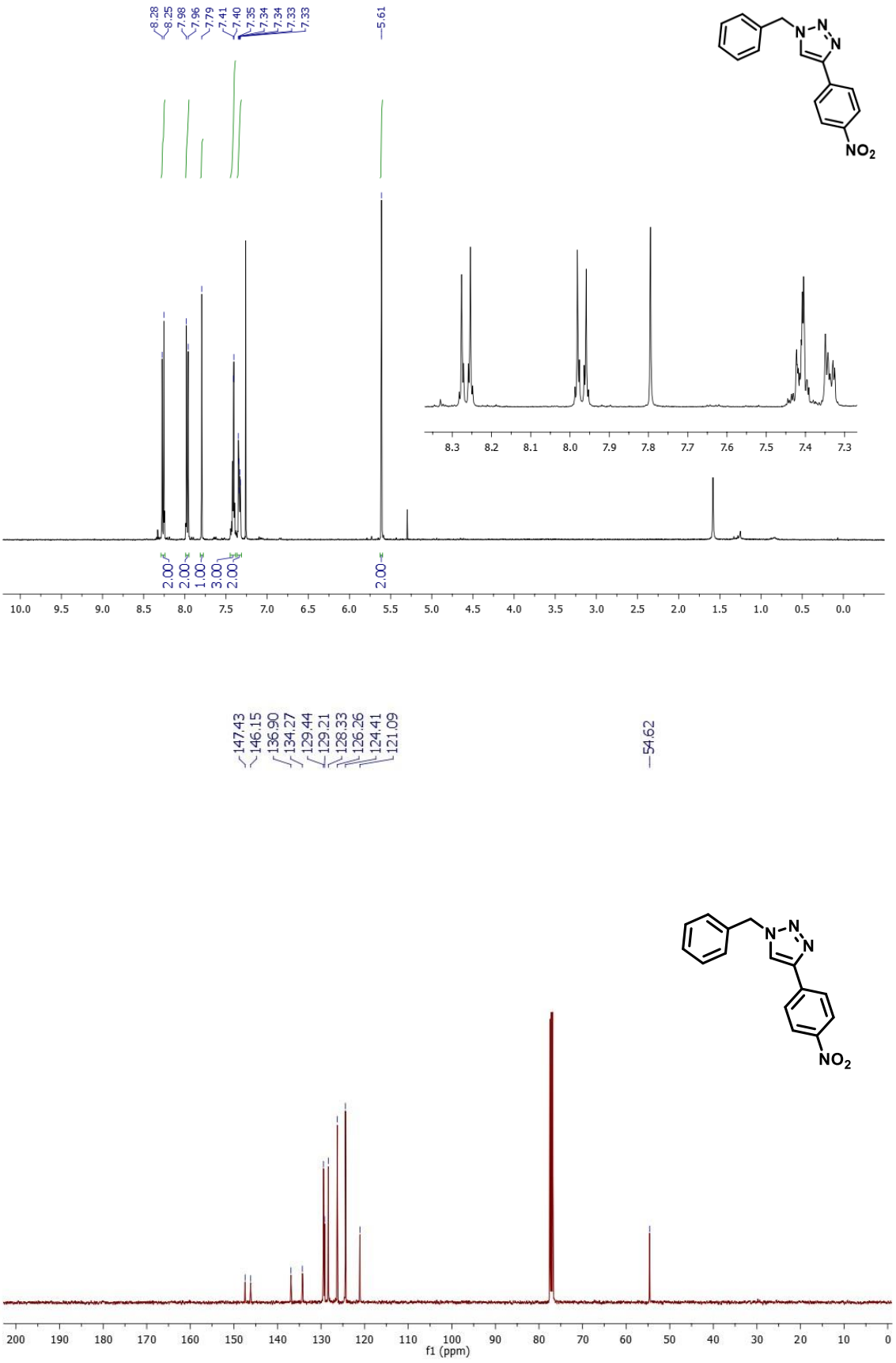

Figure 9. ^{1}H and ^{13}C NMR spectra in $CDCl_3$ of compound **3j**.

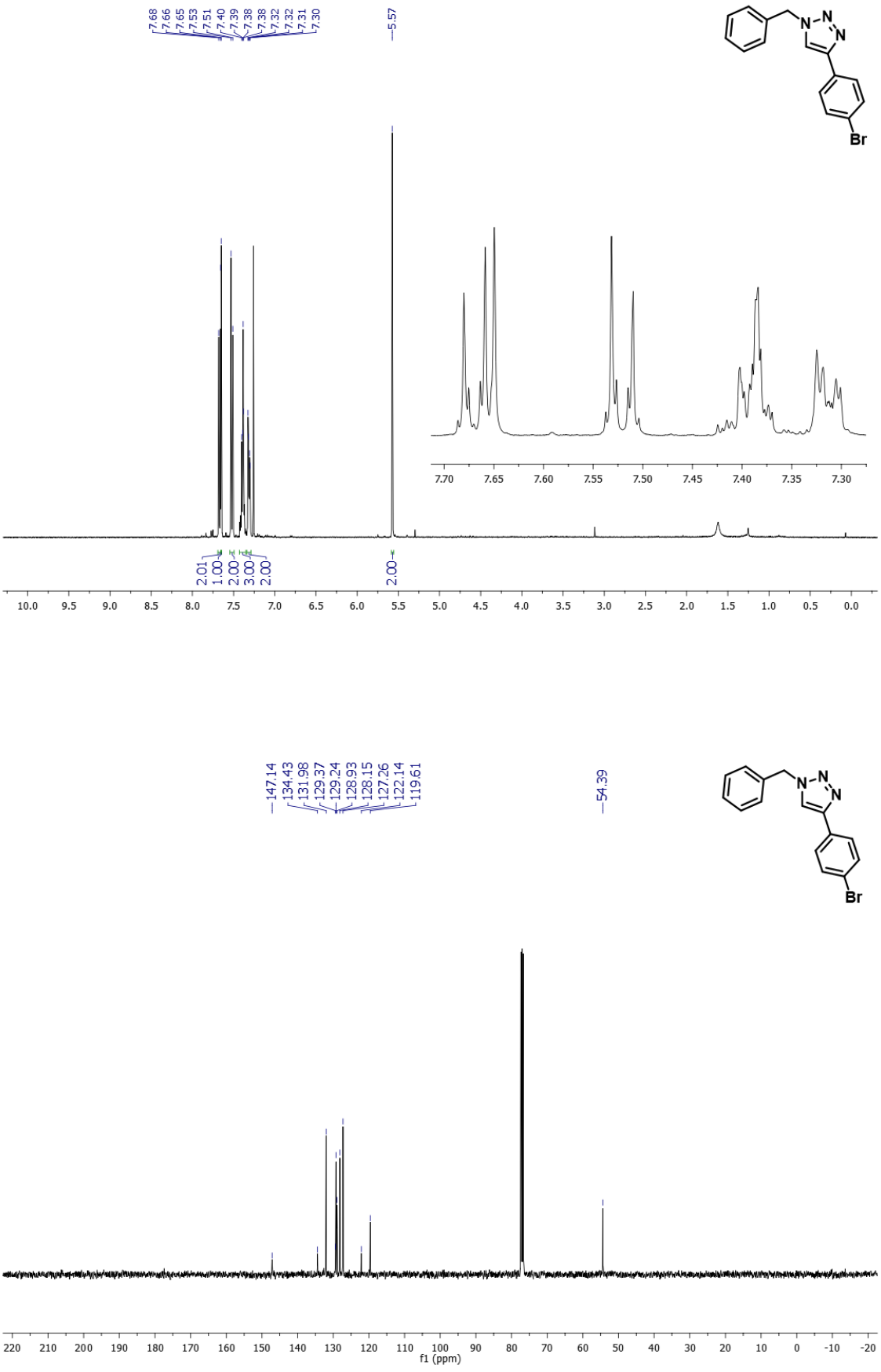

Figure 10. ^{1}H and ^{13}C NMR spectra in $CDCl_3$ of compound **3k**.

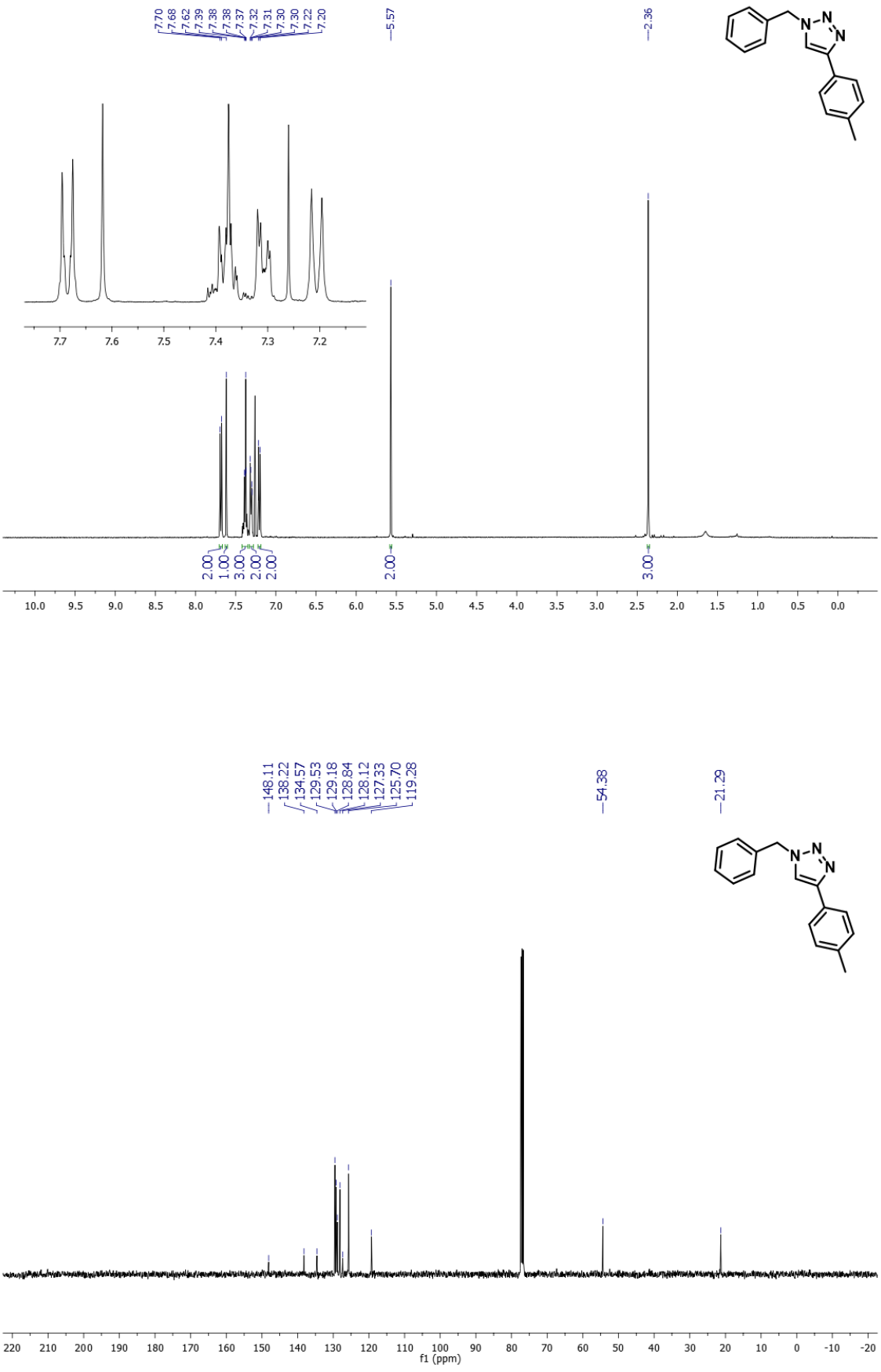

Figure 11. ^{1}H and ^{13}C NMR spectra in $CDCl_3$ of compound **3l**.

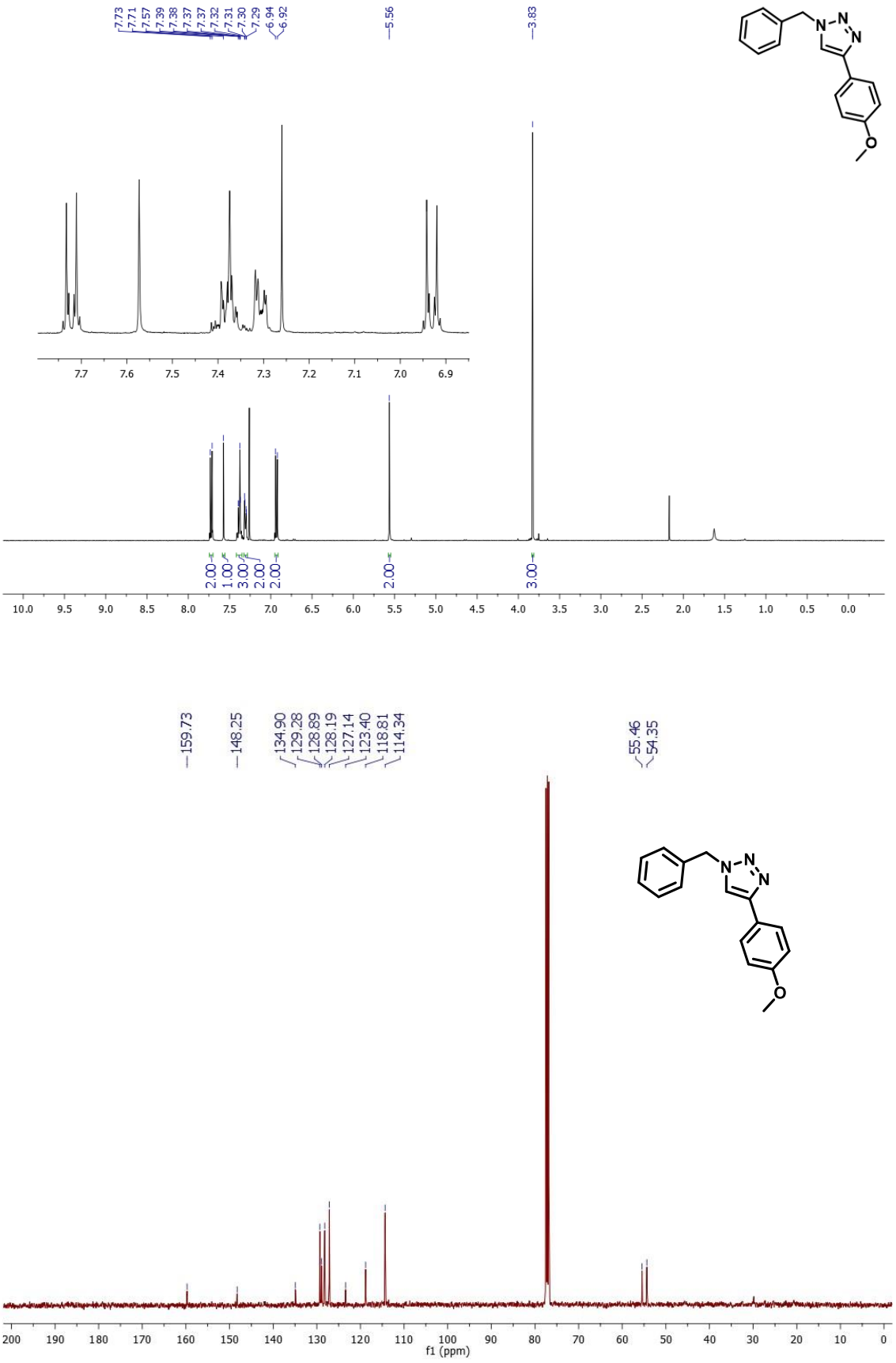

Figure 12. ^{1}H and ^{13}C NMR spectra in $CDCl_3$ of compound **3m**.

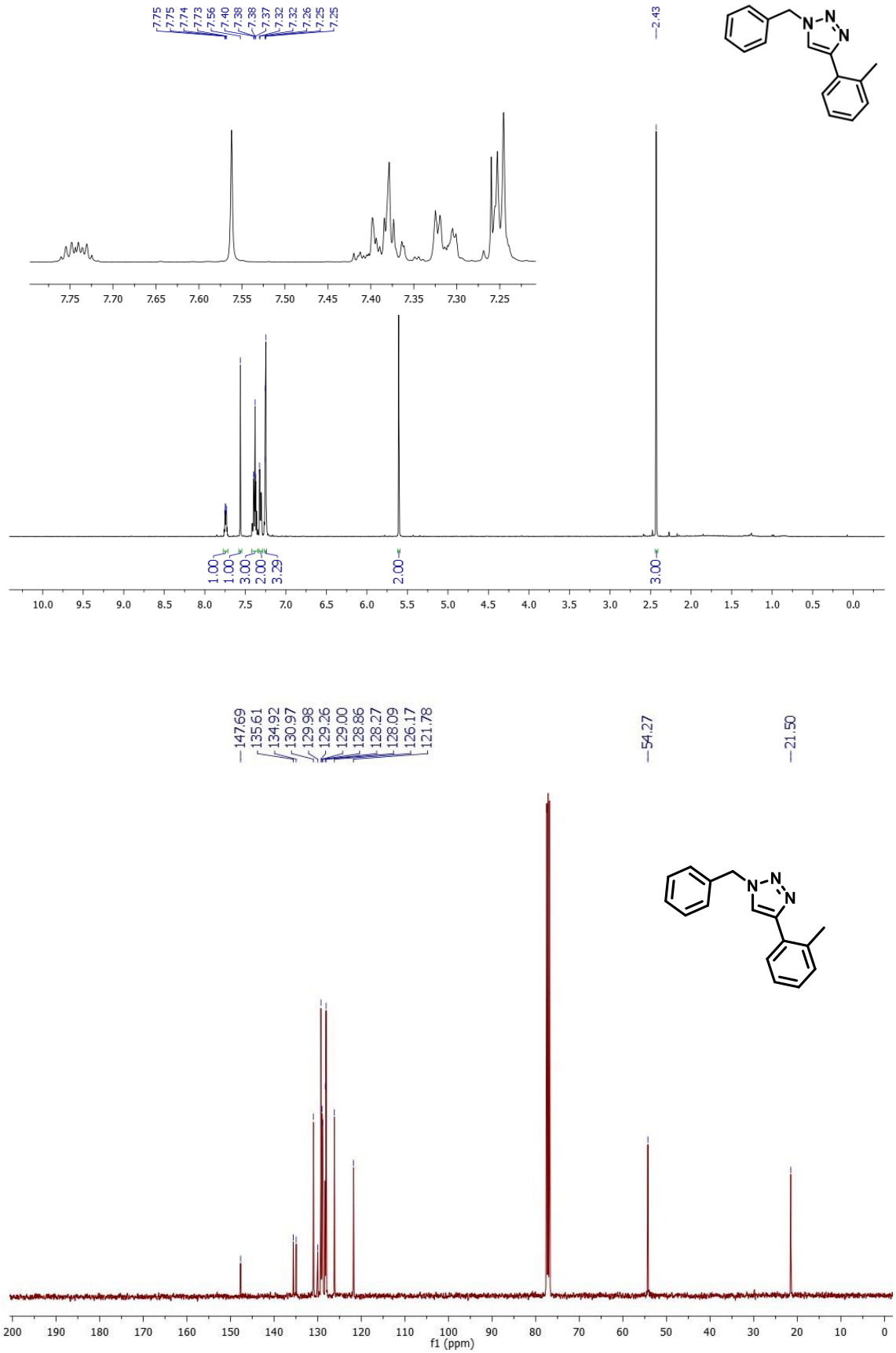

Figure 13. ^{1}H and ^{13}C NMR spectra in $CDCl_3$ of compound **3n**.

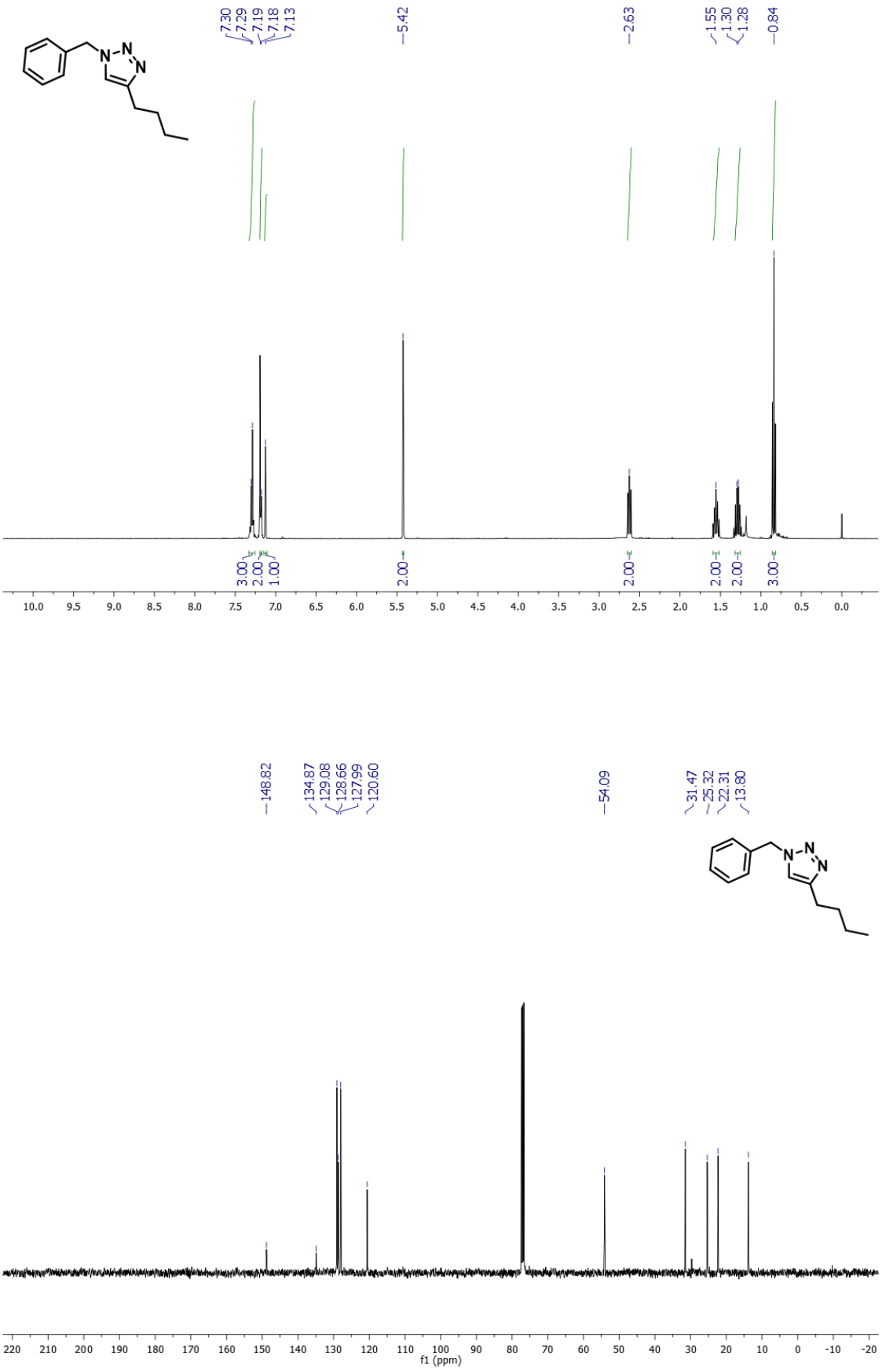

Figure 14. ^{1}H and ^{13}C NMR spectra in $CDCl_3$ of compound **3o**.

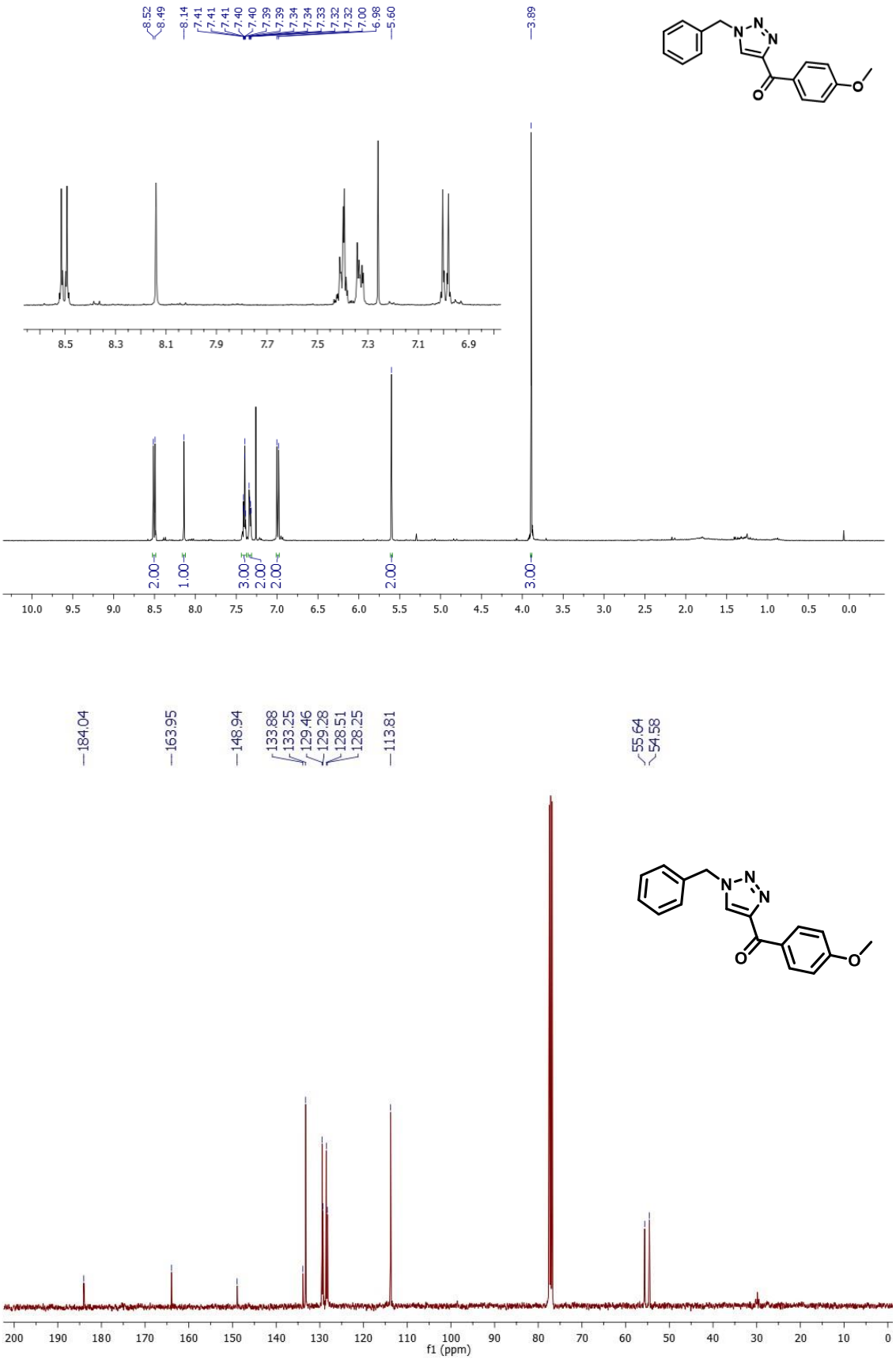

Figure 15. ^{1}H and ^{13}C NMR spectra in $CDCl_3$ of compound **3q**.